AJNR

Multiparametric Evaluation in Differentiating Glioma Recurrence from Treatment-Induced Necrosis Using Simultaneous ^{18}F-FDG-PET/MRI: A Single-Institution Retrospective Study

A. Jena, S. Taneja, A. Jha, N.K. Damesha, P. Negi, G.K. Jadhav, S.M. Verma and S.K. Sogani

AJNR Am J Neuroradiol 2017, 38 (5) 899-907
doi: https://doi.org/10.3174/ajnr.A5124
http://www.ajnr.org/content/38/5/899

Multiparametric Evaluation in Differentiating Glioma Recurrence from Treatment-Induced Necrosis Using Simultaneous ^{18}F-FDG-PET/MRI: A Single-Institution Retrospective Study

A. Jena, S. Taneja, A. Jha, N.K. Damesha, P. Negi, G.K. Jadhav, S.M. Verma, and S.K. Sogani

ABSTRACT

BACKGROUND AND PURPOSE: Differentiating glioma recurrence from treatment-induced necrosis can be a challenge on conventional imaging. This study aimed to assess the diagnostic performance of each functional MR imaging and PET parameter derived by using simultaneous FDG-PET/MR imaging individually and in combination in the evaluation of suspected glioma recurrence.

MATERIALS AND METHODS: Thirty-five treated glioma patients with 41 enhancing lesions (World Health Organization grade II = 9, III = 13, IV = 19) on MR imaging after an operation followed by radiation therapy and/or chemotherapy formed part of this study. Using PET/MR imaging, we calculated the normalized mean relative CBV, mean ADC, Cho/Cr, and maximum and mean target-to-background ratios. Statistical analysis was performed to determine the diagnostic performance of each parameter by receiver operating characteristic analysis individually and in combination with multivariate receiver operating characteristic analysis for the detection of glioma recurrence. Histopathology or clinicoradiologic follow-up was considered the criterion standard.

RESULTS: Of 35 patients, 25 (30 lesions) were classified as having a recurrence and 10 (11 lesions) patients as having treatment-induced necrosis. Parameters like $rCBV_{mean}$ (mean relative CBV), ADC_{mean}, Cho/Cr, and maximum and mean target-to-background ratios were statistically significant in the detection of recurrent lesions with an accuracy of 77.5%, 78.0%, 90.9%, 87.8%, and 87.8%, respectively. On multivariate receiver operating characteristic analysis, the combination of all 3 MR imaging parameters resulted in an area under the curve of 0.913 ± 0.053. Furthermore, an area under the curve of 0.935 ± 0.046 was obtained when MR imaging parameters (ADC_{mean} and Cho/Cr) were combined with the PET parameter (mean target-to-background ratio), demonstrating an increase in diagnostic accuracy.

CONCLUSIONS: Simultaneous PET/MR imaging with FDG offers correlative and synergistic multiparametric assessment of glioma recurrence with increased accuracy and clinical utility.

ABBREVIATIONS: AUC = area under the curve; CE = contrast-enhanced; max = maximum; rCBV = relative cerebral blood volume; ROC = receiver operating characteristic; SUV = standardized uptake value; TBR = target-to-background ratio

Glioma is currently managed by surgical resection followed by radiation therapy and/or chemotherapy, depending on the aggressiveness of the tumor. Most of these tumors, despite treatment, recur or progress during the course of the disease. Furthermore, treatment with chemoradiation therapy is associated with necrosis.[1] Up to 30% of patients with glioblastoma on chemoradiation therapy develop treatment-related effects, which mimic tumor recurrence, and both present as a new enhancing lesion on contrast-enhanced (CE) MR imaging.[2] This effect gets further complicated because recurrences most often occur within or adjacent to the primary tumor site.[3] Moreover, recurrent glioma and radiation necrosis may coexist, further obscuring this differentiation.[4] Hence, differentiation of tumor recurrence from treatment-induced necrosis, which remains a challenge on conventional CE-MR imaging,[2,5] is important because their management and prognosis are completely different.[6]

Advanced neuroimaging with MR imaging and PET has been proposed in the past for assessment of glioma recurrence.[7,8] MR imaging, besides providing superior tissue contrast, also provides functional information through perfusion, diffusion, and spectroscopy. PET imaging, on the other hand, provides additional

Received August 27, 2016; accepted after revision December 21.

From the PET SUITE (A. Jena, S.T., A. Jha, P.N.), Departments of Molecular Imaging and Nuclear Medicine, Radiation Oncology (G.K.J., S.M.V.), and Neurosurgery (N.K.D., S.K.S.), Indraprastha Apollo Hospitals, Sarita Vihar, New Delhi, India.

All procedures performed in studies involving human participants were in accordance with the ethics standards of the institutional and/or national research committee and with the 1964 Declaration of Helsinki and its later amendments or comparable ethics standards.

Please address correspondence to Amarnath Jena, DNB, PET SUITE, Department of Molecular Imaging and Nuclear Medicine, Indraprastha Apollo Hospitals, Sarita Vihar, Delhi-Mathura Rd, New Delhi, India-110076; e-mail: drjena2002@yahoo.com

http://dx.doi.org/10.3174/ajnr.A5124

information about tumor metabolism. FDG has been extensively used in the differentiation of glioma recurrence from radiation necrosis with variable results.[9] High physiologic uptake of FDG in the normal brain and its uptake in inflammatory cells often result in poor tumor-to-background differentiation and make it a moderate test for characterization of tumor recurrence.[10] This outcome has resulted in research into several more accurate PET tracers. Amino acid–based radio tracers such as ^{11}C-methionine, ^{18}F-fluoro-ethyl-tyrosine, and ^{18}F-fluoro-l-thymidine are known to offer better imaging characteristics, however, are not easily available. ^{11}C with a very short half-life needs an in-house cyclotron for production. ^{18}FDG, being a commonly available tracer with low cost suitable for wider application, formed the basis of our work. The role of CT in the diagnosis of glioma recurrence is limited, with CE-MR imaging remaining the mainstay in neuroimaging.[11] In an attempt to improve diagnostic accuracy, PET/CT has been used along with CE-MR imaging with limited success.[12] With an aim to complement information for this purpose, multiparametric assessment with various functional MR imaging parameters such as choline/creatine, choline/*N*-acetylaspartate, relative cerebral blood volume (rCBV), and apparent diffusion coefficient have been used in the past,[13,14] whereas a few studies have tried coregistration of MR imaging with PET parameters such as standardized uptake value (SUV) and target-to-background ratio (TBR) performed separately on different occasions to improve diagnostic accuracy.[12,15,16]

The advent of simultaneous PET/MR imaging has made it possible to assess all the parameters together in the same physical space in a single examination. We believe that simultaneous acquisition may help in overcoming some of the limitations of individual techniques and bring a synergistic effect in improved differentiation of recurrence from treatment-induced necrosis.

The present study aimed to assess the diagnostic performance of each of these parameters derived by using simultaneous FDG-PET/MR imaging individually and in combination by receiver operating characteristic (ROC) analysis for the evaluation of suspected glioma recurrence.

MATERIALS AND METHODS

Patients

In this retrospective study between March 2013 and September 2015, 41 consecutive patients who underwent simultaneous FDG-PET/MR imaging for glioma recurrence evaluation were chosen after obtaining prior approval of the institutional review board and signed informed consent. Inclusion criteria were histopathologic-proved glioma, previous treatment with an operation and radiation therapy with or without chemotherapy, and a high index of clinical suspicion for recurrence along with contrast enhancement on MR imaging. Exclusion criteria were nonglial primary brain tumors, proved malignancy of other sites, pregnancy, being younger than 18 years of age, standard contraindications to MR imaging, and loss of the patient to follow-up. Finally, 35 patients (6 women, 29 men; mean age, 50 ± 12 years) with 41 lesions (World Health Organization grade II = 9, III = 13, IV = 19) formed part of this study. Twenty-nine patients received chemoradiation therapy, whereas 6 patients received only radiation therapy. The interval between radiation therapy and FDG-PET/MR imaging ranged from 7 to 96 months, with a solitary case with a maximum of 233 months. The patient characteristics are available in Table 1.

Table 1: Patient characteristics

Characteristic	Value
Age (mean) (yr)	50 ± 12
Sex (No. of patients) (%)	
Male	29 (82.8)
Female	6 (17.2)
Primary histopathology (No. of lesions) (%)	
Glioblastoma	17 (41.5)
Anaplastic astrocytoma	9 (21.9)
Anaplastic oligodendroglioma	4 (9.8)
Oligodendroglioma	7 (17.1)
Others	4 (9.7)
WHO classification (No. of lesions) (%)	
Grade II	9 (22.0)
Grade III	13 (31.7)
Grade IV	19 (46.3)
Primary site of glioma (No. of lesions) (%)	
Frontal	15 (36.6)
Parietal	2 (4.9)
Temporal	10 (24.4)
Multilobar	14 (34.1)
Primary treatment (No. of patients) (%)	
Operation+radiation therapy	6 (17.2)
Operation+radiation therapy+chemotherapy	29 (82.8)
Final diagnosis (No. of lesions) (%)	
Recurrence	30 (73.2)
Histopathology	21 (51.2)
Clinicoradiologic follow-up	9 (22.0)
Treatment-induced necrosis	11 (26.8)
Histopathology	2 (4.9)
Clinicoradiologic follow-up	9 (21.9)

Note:—WHO indicates World Health Organization.

Lesion Diagnosis

A combination of clinical and imaging follow-up and histopathology was considered the criterion standard. Patients with a disease-related adverse event, progressive disease on imaging, and/or a biopsy positive for viable tumor tissue were positive for recurrence. Patients who were stable or did not show any adverse events clinically and did not progress on imaging were considered positive for treatment-induced necrosis.

Instrumentation: Simultaneous PET/MR Imaging

Simultaneous FDG-PET/MR imaging was performed on a Biograph mMR scanner (Siemens, Erlangen, Germany). This system consists of a modified 3T system (Magnetom Verio; Siemens) with a fully functional PET system, equipped with avalanche photodiode technology. The MR imaging scanner features a high-performance gradient system (45 mT/m) with a slew rate of 200 T/m/s and is equipped with total imaging matrix coil technology. The PET scanner has a spatial resolution of 4.3 mm at 1 and 5.0 mm at 10 cm from the transverse FOV; its sensitivity is 1.47% at the center of the FOV and 1.38% at 10 cm.

Imaging Protocol

The patients fasted for 6 hours before intravenous FDG injection of 352.12 ± 64.26 MBq. PET/MR imaging started 45–60 minutes after injection for 25–30 minutes of PET acquisition, during which various MR imaging sequences were performed.

A simultaneous brain PET/MR imaging protocol was composed of a transversal T1WI ultrashort TE sequence (TR/TE1/TE2, 11.94/0.07/22.46 ms) for attenuation correction and other MR imaging sequences for complete diagnostic evaluation of the brain, which included an axial FLAIR sequence (TR/TE, 7000/94 ms; TI, 2215.2 seconds; section thickness, 5 mm); a T2-weighted turbo spin-echo sequence (TR/TE, 4300/100 ms; section thickness, 5 mm); DWI (TR/TE, 4600/101 ms; $b = 0$, 400, 1000 s/mm^2); PWI/perfusion EPI (TR/TE, 2550/31 ms); and 3D-encoded MPRAGE (TR/TE/TI, 1500/2.33 ms/900 seconds; spatial resolution, $1.2 \times 1 \times 1$ mm) in the sagittal plane. In each case, 3D multivoxel ^{1}H-MR spectroscopy (TR/TE, 1510/135 ms; FOV, 120 mm; matrix, $8 \times 8 \times 8$ cm; acquisition, 1 average; scanning time, 5 minutes 41 seconds) was performed.

After the scan, all coincident data were sorted into a 2D-PET sinogram, which was subsequently reconstructed into transaxial sections, with an iterative 3D-ordered-subset expectation maximization algorithm with 3 iterations and 21 subsets, Gaussian smoothing of 4 mm in full width at half maximum, and a zoom of 1. The voxel size of brain PET images was $1.39 \times 1.39 \times 2.03$ mm. MR imaging, PET, and PET/MR imaging scans were reviewed at a syngo.via platform (Siemens) by using the mMR general workflow.

PET and MR Image Quality Control

All PET/MR imaging studies were performed by using standard imaging protocol for both PET and MR imaging, adhering to the principle of the Quantitative Imaging Biomarkers Alliance protocol and standards (https://www.rsna.org/qiba/): in case of PET, tracer dose, time delay after injection, acquisition time; and, in case of MR imaging, consistency of imaging sequences. Distortion-correction-enabled diffusion-weighed images were acquired to minimize error in the ADC calculation. For PET images, emission data were corrected for randoms, dead time, and scatter, and attenuation correction was performed by using an MR imaging–based ultrashort TE sequence.

Image Analysis

Quantitative analysis of FDG-PET/MR imaging scans was performed by a radiologist and a nuclear medicine physician in consensus, with >10 years' experience in diagnostic radiology or nuclear medicine, who were blinded to the clinical information, histopathologic data, clinicoradiologic follow-up information, and final diagnosis for each lesion.

ROI Selection

First, by subtraction of precontrast from postgadolinium T1WIs, we achieved a software-based postcontrast subtraction series wherever possible to accurately isolate areas of enhancing tumor.[17] We calculated ADC on-line by using system software, applying a monoexponential model. The most representative spectra observed within/around the lesion showing maximum PET uptake was taken for calculation of Cho/Cr.[18]

A freehand 2D ROI was drawn manually over the most representative section with maximum enhancement and was stored. This freehand ROI was duplicated by using the copy-paste function over the FDG-PET image, software generated ADC and CBV maps to find the respective maximum standardized uptake value (SUV_{max}), mean standardized uptake value (SUV_{mean}), mean ADC (ADC_{mean}), and mean CBV (CBV_{mean}) (Figs 1 and 2). Maximum target-to-background ratio (TBR_{max}), mean target-to-background ratio (TBR_{mean}), and $rCBV_{mean}$ were calculated by dividing SUV_{max}, SUV_{mean}, and CBV_{mean} obtained from the lesion ROI by the SUV_{mean}, SUV_{mean}, and CBV_{mean}, respectively, from a separate ROI drawn for normalization on normal contralateral white matter.

Statistical Analysis

Data were checked for normality by using the Shapiro-Wilk test before statistical analysis. Individual PET/MR imaging parameters were evaluated for the difference between glioma recurrence and treatment-induced necrosis by using a 2-tailed independent Student *t* test or Mann-Whitney *U* test. Optimal-threshold value, area under the curve (AUC), sensitivity, specificity, positive predictive value, negative predictive value, and accuracy were calculated by using receiver operating characteristic analysis for each of the PET/MR imaging parameters for their ability to detect recurrence. Multivariate analysis of variance was performed to check whether a combination of parameters was better than individual parameters. A multivariate ROC analysis was performed to analyze the increment offered by a combination of various parameters by conducting a logistical regression analysis to generate a combined ROC curve of different combinations of parameters. All statistical analyses were performed with the SPSS software package (Version 17.0; IBM, Armonk, New York). For all statistical tests, a P value $< .05$ was considered a significant difference.

RESULTS

Patient Information

Thirty-five patients enrolled in this retrospective study had 41 lesions for evaluation. Five patients had multicentric lesions. Histopathology after repeat operation showed viable tumor in 16 patients (21 lesions) and evidence of treatment-induced necrosis in 2 patients (2 lesions).

Eight patients (9 lesions) without histopathologic evaluation were classified as having treatment-induced necrosis based on a stable clinical state on extended follow-up periods, absence of any new neurologic symptoms, and no remarkable increase of the lesion size and/or metabolic activity observed on follow-up PET/MR imaging up to a mean period of 11.8 ± 4.5 months (range, 7–24 months). Nine patients (9 lesions) were finally classified as having recurrent brain tumors due to the development of neurologic symptoms and a progressive increase in size on CE-MR imaging (1 patient) or PET/MR imaging (8 patients) during follow-up.

Scan Information

All 35 patients underwent simultaneous FDG-PET/MR imaging. One patient did not have perfusion MR imaging; in 4 patients (5 lesions), the MR spectroscopy study was not contributory because of noisy spectra, and it was not acquired in 2 patients (3 multicentric lesions) and hence was not included in the analysis.

Among considered parameters, $rCBV_{mean}$, ADC_{mean}, Cho/Cr, TBR_{max}, and TBR_{mean} were found significant ($P < .05$) and used

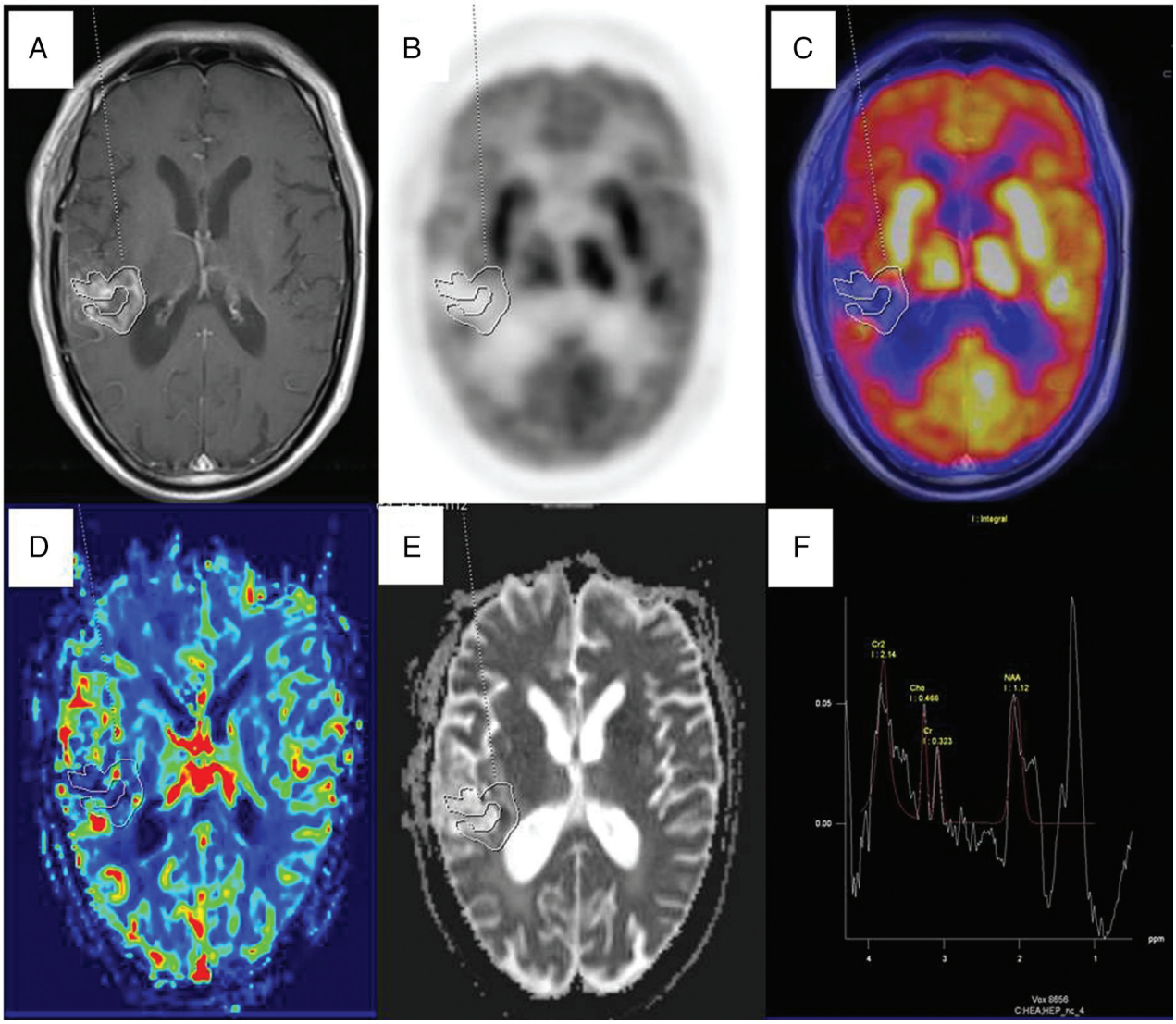

FIG 1. PET/MR imaging of a 73-year-old man with posttreatment (operation, radiation therapy, and chemotherapy) right temporoparietal glioblastoma multiforme with suspected recurrence proved to be treatment-induced necrosis on 11-month PET/MR imaging follow-up. Axial T1-weighted postcontrast image (*A*) shows an enhancing lesion along the margins of the operated bed with a freehand ROI drawn defining the enhancing component, which was copied and pasted on the FDG image (*B*), PET/MR fused image (*C*), CBV map (*D*), and ADC map (*E*) to derive SUV_{max} and SUV_{mean}, CBV_{mean}, and ADC_{mean} show no focal increased FDG uptake, CBV, and diffusion restriction on the ADC map. Multivoxel ^{1}H-MR spectroscopy (*F*) along the enhancing margin shows no increased Cho/Cr ratio.

for further combined analysis (Table 2 and Fig 3). The tumor size ranged from 0.92 to 9.5 cm^2.

Comparison of Advanced MR Imaging Parameters

PWI: $rCBV_{mean}$. In this study, $rCBV_{mean}$ was not significantly higher in patients with recurrence than in patients with treatment-induced necrosis (2.41 ± 1.02 versus 1.82 ± 1.12, $P = .082$; Fig 3*A*). However, the diagnostic accuracy of $rCBV_{mean}$ for correct identification of glioma recurrence reached 77.5% with $rCBV_{mean} \geq 1.71$ (AUC = 0.680 ± 0.111, $P = .008$), which was found to be significant (Table 2 and Fig 4*A*).

DWI: ADC_{mean}. The ADC_{mean} was significantly lower in patients with recurrence than in those with treatment-induced necrosis (1283.13 ± 210.96 versus 1558.55 ± 313.32 × $10^{-6}mm^2/s$, $P = .015$; Fig 3*B*). The diagnostic accuracy of ADC_{mean} for correct identification of glioma recurrence reached 78% with $ADC_{mean} \leq 1507 \times 10^{-6}mm^2/s$ (AUC = 0.752 ± 0.015, $P = .013$; Table 2 and Fig 4*A*).

MR Spectroscopy: Cho/Cr. Cho/Cr was significantly higher in patients with glioma recurrence than in those with treatment-induced necrosis (3.47 ± 2.20 versus 1.63 ± 0.64, $P = .002$; Fig 3*C*). The diagnostic accuracy of Cho/Cr for correct identification of glioma recurrence reached 90.9% by using Cho/Cr ≥ 1.405 (AUC = 0.861 ± 0.08, $P < .001$; Table 2 and Fig 4*A*).

Comparison of FDG Uptake Indices (TBR_{max} and TBR_{mean})

The TBR_{max} and TBR_{mean} were significantly higher in patients with glioma recurrence than in those with treatment-induced necrosis (TBR_{max}, 2.50 ± 0.97 versus 1.53 ± 0.59, $P = .001$ and TBR_{mean}, 1.70 ± 0.61 versus 0.98 ± 0.36, $P < .001$; Fig 3*D*). The diagnostic accuracy of TBR values for the correct identification of

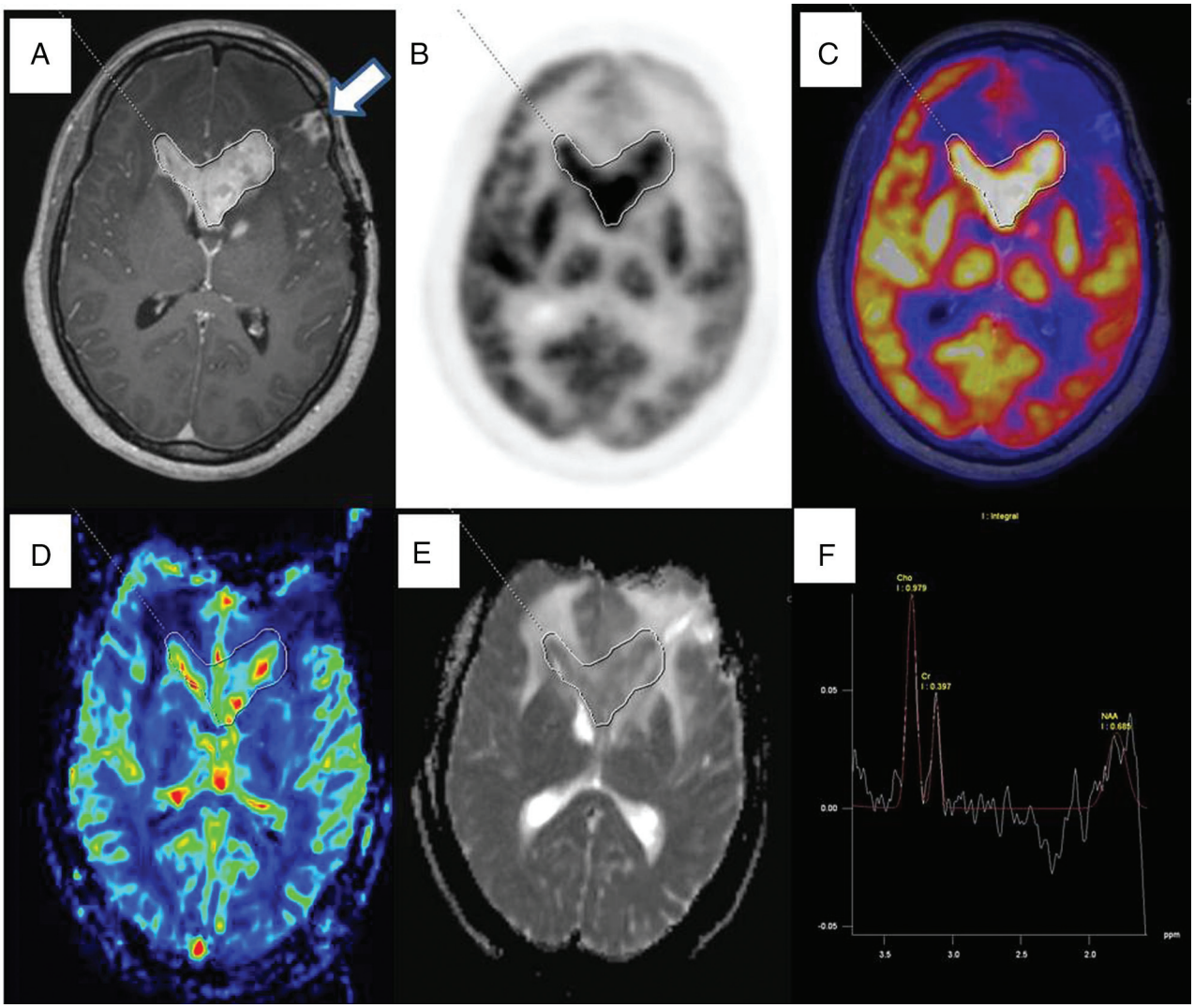

FIG 2. PET/MR images of a 49-year-old woman with posttreatment (operation and radiaton therapy) left frontotemporal anaplastic oligodendroglioma that proved to be a recurrence on histopathologic examination (glioblastoma multiforme with an oligodendroglial component; World Health Organization grade IV with a large area of necrosis). Axial T1-weighted postcontrast image (*A*) shows an enhancing lesion in the tumor bed and involving the corpus callosum. Freehand ROI drawn defining the enhancing component of the lesion and copied and pasted on the FDG image (*B*), the PET/MR fused image (*C*), the CBV map (*D*), and the ADC map (*E*) to derive SUV_{max} and SUV_{mean}, CBV_{mean}, and ADC_{mean} shows increased FDG uptake, CBV, and diffusion restriction in the ADC map. Multivoxel ^{1}H-MR spectroscopy (*F*) obtained on the FDG avid enhancing area shows an increased Cho/Cr ratio. The enhancing region anterior to the target lesion has no FDG uptake and no increased CBV, and diffusion restriction represents necrosis (*white arrow*).

Table 2: Diagnostic performance of individual parameters in the detection of glioma recurrence[a]

	$rCBV_{mean} \geq 1.709$	$ADC_{mean} \leq 1507$	$Cho/Cr \geq 1.405$	$TBR_{max} \geq 1.579$	$TBR_{mean} \geq 1.179$
Sensitivity	82.8%	86.7%	100.0%	93.3%	90.0%
Specificity	63.6%	54.5%	66.7%	72.7%	81.8%
PPV	85.7%	83.9%	88.9%	90.3%	93.1%
NPV	58.3%	60.0%	100.0%	80.0%	75.0%
Accuracy	77.5%	78.0%	90.9%	87.8%	87.8%
AUC±SE	0.68 ± 0.111	0.752 ± 0.015	0.861 ± 0.08	0.827 ± 0.078	0.888 ± 0.059
P value	.008[b]	.013[b]	<.001[b]	<.001[b]	<.001[b]

Note:—PPV indicates positive predictive value; NPV, negative predictive value; SE, standard error.

[a] The ADC_{mean} value is expressed as $\times 10^{-6} mm^2/s$ and $rCBV_{mean}$. Cho/Cr, TBR_{max}, and TBR_{mean} are ratios and hence unitless. *P* values mentioned are generated while calculating the AUC from the ROC analysis.

[b] *P* values of $rCBV_{mean}$, ADC_{mean}, Cho/Cr, TBR_{max}, and TBR_{mean} are <.05 and hence are statistically significant. *P* value reflects the significance of the ROC analysis of individual parameters represented in the table.

recurrence of brain gliomas reached 87.8% with $TBR_{max} \geq 1.58$ (AUC = 0.827 ± 0.078, $P < .001$; Table 2 and Fig. 4*C*) and also with $TBR_{mean} \geq 1.18$ (AUC = 0.888 ± 0.059, $P < .001$; Table 2 and Fig 4*C*), though with a superior AUC.

Comparison of Combined Parameters

On multivariate analysis of variance, a statistically significant difference between glioma recurrence and treatment-induced necrosis ($F_{5,26} = 5.871$, $P = .001$; Wilks $\lambda = 0.470$, partial $\eta^2 = 0.530$) was observed.

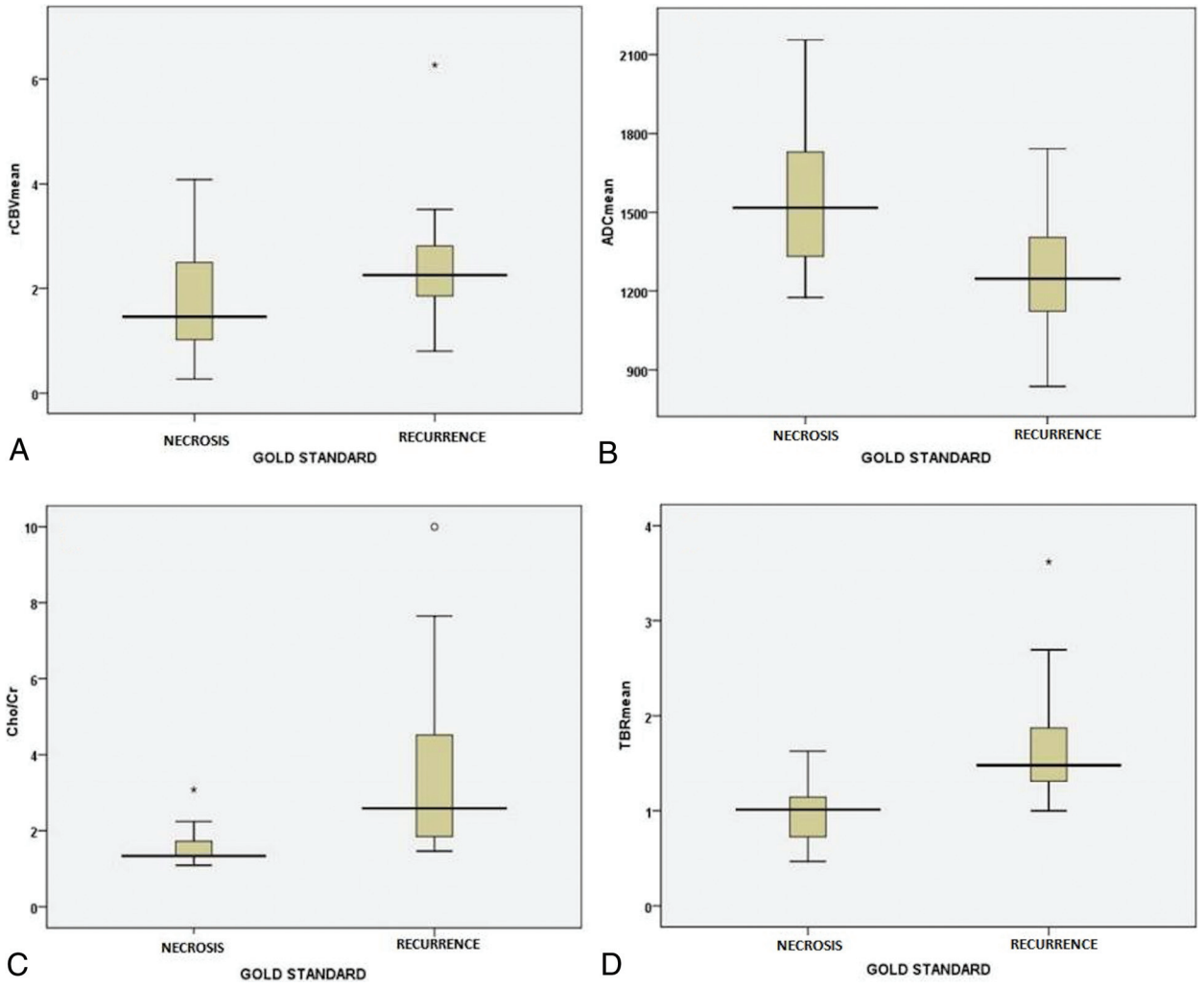

FIG 3. Box-and-whisker plots comparing $rCBV_{mean}$ (*A*), ADC_{mean} (*B*), Cho/Cr (*C*), and TBR_{mean} (*D*) between the glioma recurrence and treatment-induced necrosis. Whiskers represent the range of data; boxes represent the distance between the first and third quartiles.

Combinational Analysis

Various combinations of several parameters were performed, and multivariate ROC analysis was performed as depicted in Table 3 (Fig 4*B*, -*D*).

Combined Analysis of MR Imaging Parameters: Cho/Cr, $rCBV_{mean}$, and ADC_{mean}

Individually, Cho/Cr achieved a maximum AUC of 0.861 ± 0.080 in the detection of glioma recurrence. On multivariate ROC analysis, the addition of ADC_{mean} to either $rCBV_{mean}$ or Cho/Cr resulted in an improved diagnostic capability of both $rCBV_{mean}$ and Cho/Cr as noted by an increment in the AUC of the combinations. The combination of all 3 MR imaging parameters resulted in a combined AUC of 0.913 ± 0.053 (Table 3 and Fig 4*B*).

Combined Analysis of MR Imaging and FDG Parameters: TBR_{max}, TBR_{mean}, Cho/Cr, $rCBV_{mean}$, and ADC_{mean}

Individually, TBR_{mean} has the maximum AUC (0.888 ± 0.059) of all the MR imaging and PET parameters. Among intervariable evaluation with multivariate analysis of variance for the predictability of diagnosis, ADC_{mean} ($P = .001$) and TBR_{mean} ($P = .001$) were found to be the most significant variables in predicting glioma recurrence. On multivariate ROC analysis, the maximum AUC of 0.935 ± 0.046 was achieved with a combination of ADC_{mean}, Cho/Cr, and TBR_{mean} (Fig 4*D*). Moreover, a combination of either TBR_{max} or TBR_{mean} with ADC_{mean} and/or Cho/Cr improved the AUC value significantly beyond that of individual combining parameters (Table 3).

Summary of Results

Among all individual parameters, Cho/Cr in MR imaging and TBR_{mean} in PET are the most significant discriminators for the prediction of recurrence. Among MR imaging parameters alone, $rCBV_{mean}$ should be used in conjunction with Cho/Cr and ADC_{mean} for differentiating recurrence from treatment-induced necrosis. The maximum AUC is achieved by combining TBR_{mean}, ADC_{mean}, and Cho/Cr.

DISCUSSION

Treatment-induced necrosis is a common treatment-related morbidity in the management of gliomas, and the rate of radiation necrosis increases with incorporation of temozolomide into high-grade glioma management.[19] The differentiation of glioma

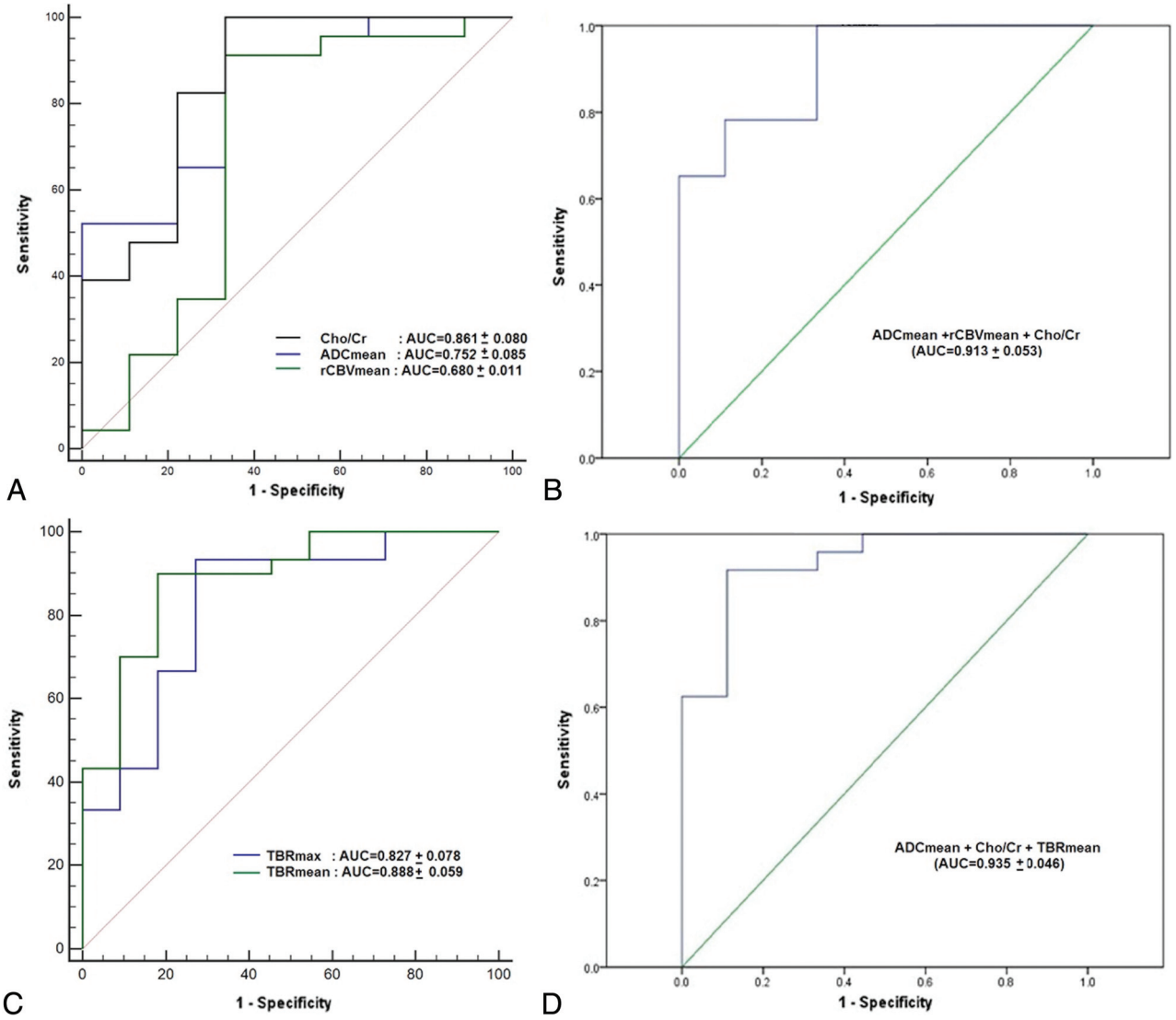

FIG 4. Receiver operating characteristic curves with their respective AUC values of MR imaging parameters (*A*) showing the high diagnostic performance of Cho/Cr in the detection of glioma recurrence. With multivariate ROC analysis, the ROC curve and AUC of all 3 MR imaging parameters combined show a significant increment in AUC over the individual MR imaging parameters (*B*). ROC curves with their respective AUC values of FDG parameters (*C*) show the high diagnostic performance of TBR_{mean} in the detection of glioma recurrence. Multivariate ROC analysis, ROC curve, and AUC of the best performing FDG-PET/MR imaging combination of ADC_{mean}, Cho/Cr, and TBR_{mean} show a significant increment over individual MR imaging or PET parameters (*D*).

Table 3: Multivariate ROC analysis showing AUC ± SE values for various combinations of FDG-PET and MRI parameters in the detection of glioma recurrence[a]

	$rCBV_{mean}$ (0.680 ± 0.011)	ADC_{mean} (0.752 ± 0.085)	Cho/Cr (0.861 ± 0.080)	ADC_{mean} + $rCBV_{mean}$ (0.781 ± 0.079)	ADC_{mean} + Cho/Cr (0.912 ± 0.051)	$rCBV_{mean}$ + Cho/Cr (0.860 ± 0.083)	ADC_{mean} + $rCBV_{mean}$ + Cho/Cr (0.913 ± 0.053)
ADC_{mean} (0.752 ± 0.085)	0.781 ± 0.079						
Cho/Cr (0.861 ± 0.080)	0.860 ± 0.083	0.912 ± 0.051		0.913 ± 0.053[b]			
TBR_{max} (0.827 ± 0.078)	0.831 ± 0.081	0.848 ± 0.072	0.894 ± 0.059	0.850 ± 0.073	0.935 ± 0.044	0.889 ± 0.061	0.932 ± 0.046
TBR_{mean} (0.888 ± 0.059)	0.884 ± 0.063	0.888 ± 0.058	0.935 ± 0.044	0.897 ± 0.057	0.935 ± 0.046[b,c]	0.928 ± 0.047	0.932 ± 0.048[b]

[a] Each entry represents the AUC ± SE of a combination of parameters mentioned in the respective rows and columns. Values in parentheses represent AUC ± SE of that particular parameter or combination. Blank cells are left to avoid repetition of values.

[b] A combination of FDG-PET and MR imaging parameters has a better AUC ± SE than a combination of MR imaging parameters.

[c] Note that the maximum AUC was achieved with a combination of ADC_{mean}, Cho/Cr, and TBR_{mean}.

recurrence or progression from radiation injury can be a radiologic dilemma, irrespective of the imaging technique used.[20]

It is known that functional imaging methods complement anatomic information and yield different aspects of pathophysiology. The combination of PET and CE-MR imaging information with retrospective fusion has been reported to increase diagnostic accuracy over any single technique.[12,15,16] In an integrated PET/MR system, PET and MR imaging information are not only combined but an additional value is expected owing to co-interpretation of both the signals.[21]

In our study, the results derived from individual PET and functional MR imaging parameters from simultaneously ac-

quired FDG-PET/MR imaging are in agreement with the published literature.

With an optimized threshold of 1507 × 10^{-6}mm^2/s for ADC_{mean}, an AUC of 0.752 ± 0.015 was obtained, which is close to the reported threshold of 1490 × 10^{-6}mm^2/s and AUC of 0.779.[22] We achieved an accuracy of 77.5% and an AUC of 0.68 ± 0.111 with an optimized threshold of 1.709 for $rCBV_{mean}$. Our calculated sensitivity and specificity of 82.8% and 63.6% are similar to 86% and 70%, respectively, reported with a comparatively lower threshold of 1.3.[23] However, wide variation has been reported in rCBV thresholds to detect recurrence,[24] and reasons ascribed include rapid extravasation of gadolinium-based contrast agent and vascular leak in the irradiated bed, especially with chemoradiation therapy.[25] With an optimized threshold of 1.405 for Cho/Cr, we achieved an accuracy and AUC of 90.9% and 0.861 ± 0.080, respectively, which are in concordance with the reported values of 93.1% and 0.913, respectively, with 1.54 as a threshold.[26] FDG-PET has been used to detect glioma recurrence with a varied range of reported sensitivities from 43% to 95% and specificities from 50% to 100%.[9] Despite known limitations of FDG in the detection of glioma recurrence of any histology, a recent meta-analysis of FDG found a respectable pooled AUC of 0.866 ± 0.034 for FDG-PET.[9] We achieved an AUC of 0.888 ± 0.059 by using an optimized threshold of 1.18 for TBR_{mean} in the detection of glioma recurrence that is in agreement with the reported AUC of 0.898 by Nozawa et al[16] in the differentiation of recurrent/residual high-grade glioma from posttreatment changes or low-grade glioma, however, by using TBR_{max} with a threshold of 1.8.

Because there is no single technique that can solve this clinical dilemma, researchers have attempted to combine functional MR imaging parameters to achieve an improved diagnostic accuracy beyond any single parameter.[13,27]

Moreover, in the past, retrospective fusion of FDG-PET with CE-MR imaging has aided in improved differentiation of glioma recurrence qualitatively, compared with FDG-PET or MR imaging alone.[12,15,16] In a group of 30 patients with high-grade gliomas, Estrada et al[12] reported an accuracy of 73% for FDG-PET, which improved to 93% with visual qualitative analysis of fused FDG-PET with CE-MR imaging.

Matsusue et al,[27] with a semi-quantitative multiparametric scoring system for ADC ratio, rCBV, Cho/Cr, and Cho/NAA in 15 patients, reported an accuracy of 93.3% in the detection of glioma recurrence. We achieved an AUC of 0.913 ± 0.053 by combining ADC_{mean}, $rCBV_{mean}$, and Cho/Cr by multivariate ROC analysis.

Our quantitative analysis of combined parameters also supports this body of evidence. We observed that combinations of individual parameters demonstrate superior results in comparison with individual parameters. We achieved an AUC of 0.913 ± 0.053 when all MR imaging parameters were combined, which further improved to 0.932 ± 0.046 when TBR_{max} or TBR_{mean} was added, clearly highlighting the utility of combinational analysis. However, the highest AUC of 0.935 ± 0.046 was achieved by combining ADC_{mean}, Cho/Cr, and TBR_{mean}.

We found that a simultaneous PET/MR imaging study offers advantages such as being logistically simple, implying, thereby, that it is performed as a single examination to obtain PET and MR imaging datasets; reduced examination time, thereby improving patient compliance; and correlative image reading and interpretation, which could help in localizing the most suspicious area on the PET image in voxel selection for MR spectroscopy. Furthermore, as observed by Mong et al,[28] we also found that PET uptake could help in accurate classification of suspicious ADC lesions. In the present study, we used an ultrashort TE sequence for MR imaging–based attenuation correction for brain PET, which is reported to result in accurate quantification of PET parameters,[29] more importantly offering comparable accuracy of CT-based attenuation correction.

Our study has several limitations. It is a retrospective study with a small group and a relatively heterogeneous class of patients to perform robust statistical analysis. The present study only provides within-sample prediction characteristics and is not adequately sized to provide a decent out-of-sample prediction. Although desirable, histologic diagnosis in all the lesions could not be obtained due to ethical concerns associated with high morbidity and sampling error.[30]

Hence, further large-scale prospective multicentric trials are required with simultaneous PET/MR imaging and FDG, a commonly available radiotracer, to validate our results.

CONCLUSIONS

Simultaneous PET/MR imaging with FDG offers correlative and synergistic multiparametric assessment of glioma recurrence with increased accuracy and clinical utility.

ACKNOWLEDGMENTS

We thank Dr Aru Singh for technical help in the statistical analysis.

REFERENCES

1. Chamberlain MC, Glantz MJ, Chalmers L, et al. **Early necrosis following concurrent Temodar and radiotherapy in patients with glioblastoma.** *J Neurooncol* 2007;82:81–83 CrossRef Medline
2. Brandes AA, Franceschi E, Tosoni A, et al. **MGMT promoter methylation status can predict the incidence and outcome of pseudoprogression after concomitant radiochemotherapy in newly diagnosed glioblastoma patients.** *J Clin Oncol* 2008;26:2192–97 CrossRef Medline
3. Chan JL, Lee SW, Fraass BA, et al. **Survival and failure patterns of high-grade gliomas after three-dimensional conformal radiotherapy.** *J Clin Oncol* 2002;20:1635–42 CrossRef Medline
4. Sugahara T, Korogi Y, Tomiguchi S, et al. **Posttherapeutic intraaxial brain tumor: the value of perfusion-sensitive contrast-enhanced MR imaging for differentiating tumor recurrence from nonneoplastic contrast-enhancing tissue.** *AJNR Am J Neuroradiol* 2000;21:901–09 Medline
5. Brandsma D, Stalpers L, Taal W, et al. **Clinical features, mechanisms, and management of pseudoprogression in malignant gliomas.** *Lancet Oncol* 2008;9:453–61 CrossRef Medline
6. Alexiou GA, Tsiouris S, Kyritsis AP, et al. **Glioma recurrence versus radiation necrosis: accuracy of current imaging modalities.** *J Neurooncol* 2009;95:1–11 CrossRef Medline
7. Heiss W, Raab P, Lanfermann H. **Multimodality assessment of brain tumors and tumor recurrence.** *J Nucl Med* 2011;52:1585–600 CrossRef Medline
8. Keunen O, Taxt T, Grüner R, et al. **Multimodal imaging of gliomas in the context of evolving cellular and molecular therapies.** *Adv Drug Deliv Rev* 2014;76:98–115 CrossRef Medline
9. Wang X, Hu X, Xie P, et al. **Comparison of magnetic resonance**

spectroscopy and positron emission tomography in detection of tumor recurrence in posttreatment of glioma: a diagnostic meta-analysis. *Asia Pac J Clin Oncol* 2015;11:97–105 CrossRef Medline
10. Nihashi T, Dahabreh IJ, Terasawa T. **Diagnostic accuracy of PET for recurrent glioma diagnosis: a meta-analysis.** *AJNR Am J Neuroradiol* 2013;34:944–50, S1–11 CrossRef Medline
11. Huang RY, Neagu MR, Reardon DA, et al. **Pitfalls in the neuroimaging of glioblastoma in the era of antiangiogenic and immuno/targeted therapy: detecting illusive disease, defining response.** *Front Neurol* 2015;6:33 CrossRef Medline
12. Estrada G, González-Maya L, Celis-López MA, et al. **Diagnostic approach in suspected recurrent primary brain tumors using (18)FDG-PET/MRI, perfusion MRI, visual and quantitative analysis, and three dimensional stereotactic surface projections: first experience in Mexico.** *Rev Esp Med Nucl* 2008;27:329–39 CrossRef Medline
13. Seeger A, Braun C, Skardelly M, et al. **Comparison of three different MR perfusion techniques and MR spectroscopy for multiparametric assessment in distinguishing recurrent high-grade gliomas from stable disease.** *Acad Radiol* 2013;20:1557–65 CrossRef Medline
14. Di Costanzo A, Scarabino T, Trojsi F, et al. **Recurrent glioblastoma multiforme versus radiation injury: a multiparametric 3-T MR approach.** *Radiol Med* 2014;119:616–24 CrossRef Medline
15. Enslow MS, Zollinger LV, Morton KA, et al. **Comparison of 18F-fluorodeoxyglucose and 18F-fluorothymidine PET in differentiating radiation necrosis from recurrent glioma.** *Clin Nucl Med* 2012; 37:854–61 CrossRef Medline
16. Nozawa A, Rivandi AH, Kanematsu M, et al. **Glucose-corrected standardized uptake value in the differentiation of high-grade glioma versus post-treatment changes.** *Nucl Med Commun* 2015;36:573–81 CrossRef Medline
17. Ellingson BM, Kim HJ, Woodworth DC, et al. **Recurrent glioblastoma treated with bevacizumab: contrast-enhanced T1-weighted subtraction maps improve tumor delineation and aid prediction of survival in a multicenter clinical trial.** *Radiology* 2014;271:200–10 CrossRef Medline
18. Kim ES, Satter M, Reed M, et al. **A novel, integrated PET-guided MRS technique resulting in more accurate initial diagnosis of high-grade glioma.** *Neuroradiol J* 2016;29:193–97 CrossRef Medline
19. Peca C, Pacelli R, Elefante A, et al. **Early clinical and neuroradiological worsening after radiotherapy and concomitant temozolomide in patients with glioblastoma: tumour progression or radionecrosis?** *Clin Neurol Neurosurg* 2009;111:331–34 CrossRef Medline
20. Hygino Da Cruz LC, Rodriguez I, Domingues RC, et al. **Pseudoprogression and pseudoresponse: imaging challenges in the assessment of posttreatment glioma.** *AJNR Am J Neuroradiol* 2011;32: 1978–85 CrossRef Medline
21. Garibotto V, Heinzer S, Vulliemoz S, et al. **Clinical applications of hybrid PET/MRI in neuroimaging.** *Clin Nucl Med* 2013;38:e13–18 CrossRef Medline
22. Prager AJ, Martinez N, Beal K, et al. **Diffusion and perfusion MRI to differentiate treatment-related changes including pseudoprogression from recurrent tumors in high-grade gliomas with histopathologic evidence.** *AJNR Am J Neuroradiol* 2015;36:877–85 CrossRef Medline
23. Ozsunar Y, Mullins ME, Kwong K, et al. **Glioma recurrence versus radiation necrosis? A pilot comparison of arterial spin-labeled, dynamic susceptibility contrast enhanced MRI, and FDG-PET imaging.** *Acad Radiol* 2010;17:282–90 CrossRef Medline
24. Deng SM, Zhang B, Wu YW, et al. **Detection of glioma recurrence by ^{11}C-methionine positron emission tomography and dynamic susceptibility contrast-enhanced magnetic resonance imaging: a meta-analysis.** *Nucl Med Commun* 2013;34:758–66 CrossRef Medline
25. Gahramanov S, Raslan AM, Muldoon LL, et al. **Potential for differentiation of pseudoprogression from true tumor progression with dynamic susceptibility-weighted contrast-enhanced magnetic resonance imaging using ferumoxytol vs. gadoteridol: a pilot study.** *Int J Radiat Oncol Biol Phys* 2011;79:514–23 CrossRef Medline
26. Fink JR, Carr RB, Matsusue E, et al. **Comparison of 3 Tesla proton MR spectroscopy, MR perfusion and MR diffusion for distinguishing glioma recurrence from posttreatment effects.** *J Magn Reson Imaging* 2012;35:56–63 CrossRef Medline
27. Matsusue E, Fink JR, Rockhill JK, et al. **Distinction between glioma progression and post-radiation change by combined physiologic MR imaging.** *Neuroradiology* 2010;52:297–306 CrossRef Medline
28. Mong S, Ellingson BM, Nghiemphu PL, et al. **Persistent diffusion-restricted lesions in bevacizumab-treated malignant gliomas are associated with improved survival compared with matched controls.** *AJNR Am J Neuroradiol* 2012;33:1763–70 CrossRef Medline
29. Werner P, Rullmann M, Bresch A, et al. **Impact of attenuation correction on clinical [(18)F]FDG brain PET in combined PET/MRI.** *EJNMMI Res* 2016;6:47 CrossRef Medline
30. McGirt MJ, Woodworth GF, Coon AL, et al. **Independent predictors of morbidity after image-guided stereotactic brain biopsy: a risk assessment of 270 cases.** *J Neurosurg* 2005;102:897–901 CrossRef Medline